Human Molecular Genetics, 2007, Vol. 16, No. 9 **1039–1050**
doi:10.1093/hmg/ddm049
Advance Access published on March 6, 2007

RCAN1 (*DSCR1*) increases neuronal susceptibility to oxidative stress: a potential pathogenic process in neurodegeneration

Sílvia Porta[1,†], Selma A. Serra[3,†], Meritxell Huch[1], Miguel A. Valverde[3], Franc Llorens[2], Xavier Estivill[1], Maria L. Arbonés[1] and Eulàlia Martí[1,*]

[1]Genes and Disease Program, [2]Bioinformatics and Genomics Program, Center for Genomic Regulation (CRG-UPF), Biomedical Research Park Building, E-08003 Barcelona, Catalonia, Spain and [3]Molecular Physiology and Channelopathies, Universitat Pompeu Fabra, Barcelona, Catalonia, Spain

Received November 27, 2006; Revised February 19, 2007; Accepted February 28, 2007

Oxidative stress (OS) underlies neuronal dysfunction in many neurodegenerative disorders. Regulator of Calcineurin 1 (*RCAN1* or *DSCR1*) is a dose-sensitive gene whose overexpression has been linked to Down syndrome (DS) and Alzheimer's disease (AD) neuropathology and to the response of cells to stress stimuli. Here, we show that RCAN1 mRNA and protein expression are sensitive to OS in primary neurons, and we evaluate the involvement of RCAN1 dosage in neuronal death induced by OS. We find that *Rcan1*$^{-/-}$ neurons display an increased resistance to damage by H_2O_2, which can be reverted by *RCAN1* overexpression or by exogenous inhibitors of calcineurin. Although increased intracellular Ca^{2+} concentration is an important factor in OS-mediated cell death, our results show that Ca^{2+} loading after exposure to H_2O_2 was similar in *Rcan1*$^{+/+}$ and *Rcan1*$^{-/-}$ neurons. Our data further suggest that CaN and NFAT signaling protect against OS in both *Rcan1*$^{+/+}$ and *Rcan1*$^{-/-}$ neurons. To explain the observed differential vulnerability, we therefore propose a mechanism downstream of H_2O_2-mediated Ca^{2+} entry, involving calcineurin-NFAT signaling. These findings highlight the importance of RCAN1 gene dosage in the modulation of cell survival and death pathways and suggest that changes in the amount of RCAN1 could represent an important mechanism for regulating susceptibility to neurodegeneration, especially in DS and AD.

INTRODUCTION

RCAN1 (*regulator of calcineurin* 1, also known as CALP1, MCIP1 and Adapt78) belongs to a highly conserved family of proteins that modulate the activity of calcineurin (CaN) (1–4). CaN is a serine/threonine phosphatase which is extremely abundant in the brain and is regulated by Ca^{2+} and calmodulin. CaN modulates many Ca^{2+}-mediated responses, including neurotransmitter release, cytoskeletal stabilization, long-term memory, neurite extension and apoptosis [see (5) for a review]. The endogenous CaN regulator RCAN1 is thus relevant to the control of physiological and pathological CaN-dependent processes.

The gene encoding RCAN1, *RCAN1*—originally named *DSCR1* (*Down Syndrome Candidate Region gene 1*)—is located on human chromosome 21 (6). *RCAN1* is mostly expressed in brain and skeletal and cardiac muscle (7,8). The *RCAN1* gene contains seven exons, and differential promotor usage and first exon choice can generate several transcripts (7,9). The different mRNAs contain one of four possible initial exons (E1 through E4) and the three exons (E5 through E7) common to all forms of *RCAN1* mRNA (7). There are two main protein isoforms of RCAN1, which differ in their N-terminal regions (7): the long isoform (RCAN1L), with 252 amino acids, is encoded by the *RCAN1.1* mRNA (10); and the 197 amino-acid short isoform (RCAN1S) is encoded by the *RCAN1.4* transcript. *RCAN1.4* expression is induced by Ca^{2+} via a mechanism that depends on CaN activity. This finding suggested that RCAN1 might participate in a negative feedback loop to

*To whom correspondence should be addressed at: Genes and Disease Program, Genomic Regulation Center (CRG-UPF), Biomedical Research Park, C/Dr Aiguader 88, E-08003 Barcelona, Catalonia, Spain. Tel: +34 933160201; Fax: +34 933160099; Email: eulalia.marti@crg.es
†The authors wish it to be known that, in their opinion, the first two authors should be regarded as joint First Authors.

control CaN activity (9). In addition, *RCAN1.1* expression has been recently shown to be up-regulated by glucocorticoids (11) and down-regulated by Notch signaling (12). The mouse ortholog maps to chromosome 16 and has a similar genomic structure (13). Transcripts containing the mouse equivalents of human exons 1 and 4 respectively give rise to the expression of the long and short mouse RCAN1 isoforms.

The first indication that *RCAN1* might play a central role in pathological processes was the finding that mammalian cells increase *RCAN1* expression after exposure to damaging stimuli associated with Ca^{2+} overloading, such as oxidative stress (OS) (14–16). Interest in RCAN1 was reinforced by the discoveries that *RCAN1* transcripts are overexpressed in the brains of Down syndrome (DS) fetuses (2) and that *RCAN1* transcript and protein are both increased in the brains of individuals with Alzheimer's disease (AD) (17,18). It has been proposed that long-term or chronic induction of *RCAN1* might be associated with neurodegeneration in AD and DS, whereas short-term induction might protect cells against stress-induced damage (19,20). The detrimental consequences of RCAN1 overexpression have been analyzed in cultured primary neurons, and include the formation of microtubule-dependent aggregosome-like inclusion bodies, as well as synaptic impairment (21). Altered synaptic transmission also underlies the severe learning defects seen with modifications in the gene dosage of *nebula*, the *Drosophila* ortholog of *RCAN1* (22). Moreover, the correct dosage of *nebula* is essential for the maintenance of mitochondrial function, which has important implications in the context of OS (23).

The possible involvement of RCAN1 in OS-related signaling mechanisms is especially relevant in the context of neurodegenerative diseases, where OS is the common hallmark of progression toward loss of neuronal function. Although the published data clearly indicate that increased RCAN1 gene dose underlies neuronal dysfunction, little is known about the involvement of RCAN1 in OS-mediated neuronal death. In the present study, we have analyzed susceptibility to OS and related intracellular signaling mechanisms in primary neuronal cell cultures expressing different amounts of RCAN1. Our results show a mechanistic link between RCAN1 dose and neuronal viability in response to OS, thus suggesting that the amount of RCAN1 has a significant role in modulating signaling pathways underlying the balance between neuronal death and survival.

RESULTS

Expression of RCAN1 by primary neurons is sensitive to OS

Primary neurons obtained from mouse cerebellar cortex at early postnatal time-points were chosen for the present study, since they are a very homogeneous population of neuronal granule cells, and have been widely used as a model to dissect mechanisms of neuronal death. Moreover, *Rcan1* transcripts are abundantly expressed in the cerebellar cortex in adult and early postnatal mice (8).

Since previous studies in established human cell lines have shown increased *RCAN1* mRNA expression in response to reactive oxygen species (ROS) (14,16), we first examined whether OS could induce *Rcan1* transcription in mouse primary neurons. Exposure of cells to H_2O_2 specifically induced expression of *Rcan1.4*, but not *Rcan1.1*, 4 h after treatment (Fig. 1A). No significant changes in *Rcan1.4* mRNA expression were detected at earlier time points (data not shown). Previous reports have shown that *Rcan1.4* induction in other experimental situations occurs via a Ca^{2+}/CaN-dependent mechanism involving *Rcan1.4* promoter regions that contain NFAT transcription-factor binding motifs (2,9,24). To determine the involvement of CaN in *Rcan1.4* mRNA induction in our experimental system, neurons were pre-incubated with the CaN inhibitors cyclosporine A (CsA) and FK506. The inhibitors were used in combination because both drugs are required in primary neurons to form enough inhibitory complexes to neutralize CaN (25,26). Pre-incubation with CsA and FK506 largely prevented *Rcan1.4* induction, suggesting that this process is highly dependent on CaN activity (Fig. 1A).

Protein expression was analyzed with antibodies recognizing the C-terminal region common to RCAN1L and RCAN1S isoforms. Indirect immunofluorecence revealed a major cytoplasmic accumulation of RCAN1 in primary granular cells, with the protein homogeneously distributed both in the soma and in neuronal projections (Fig. 1B). Signal, in the form of coarse granules in the somatic cytoplasm, was detected 3,5 h min after exposure to 50 μM H_2O_2 and was maintained throughout the treatment; there was no obvious translocation to the nuclear compartment even after prolonged exposure to H_2O_2 for 5 h (Fig. 1B).

Western blot analysis revealed that RCAN1L is much more abundantly expressed than RCAN1S in primary neuronal cells (Fig. 1C, lane 1). Both RCAN1L and RCAN1S appeared as doublets, which represent differentially phosphorylated forms (10,27,28). The amount of RCAN1 decreased notably between 4 and 5 h after exposure to H_2O_2 (Fig. 1C, lanes 6–7). Interestingly, the band corresponding to hypophosphorylated RCAN1L was consistently more resistant to fading, suggesting an increased half-life. The loss of RCAN1 was accompanied by a concomitant appearance of immunoreactive bands around 30 kDa (Fig. 1C, lanes 5–7). We hypothesized that these RCAN1 degradation products might be produced by the action of the protease calpain, since calpain is activated by OS (29) and can cleave RCAN1S *in vitro* (30). Moreover, one of the calpain cleavage sites in RCAN1S also occurs in RCAN1L, suggesting that both RCAN1 forms will be susceptible to calpain proteolysis *in vivo*. Pre-incubation of primary neurons with calpain inhibitors I and II prevented the decline in expression of both RCAN1L and RCAN1S and the formation of the 30 kDa RCAN1 degradation products (Fig. 1D, compare lanes 3–4 and 5–6), indicating calpain-mediated degradation of RCAN1 after OS. In addition, calpain inhibition increased the basal accumulation of both RCAN1 isoforms (Fig. 1D, lane 2). This effect, which was more apparent with RCAN1S, suggests that calpain also regulates RCAN1 half-life in the absence of stress stimuli.

In light of reported crosstalk between CaN and calpain activities (31), we wondered whether CaN would affect RCAN1 accumulation. To test this, we pre-incubated primary neurons with CsA and FK506 before adding H_2O_2. This pre-treatment resulted in enhanced RCAN1

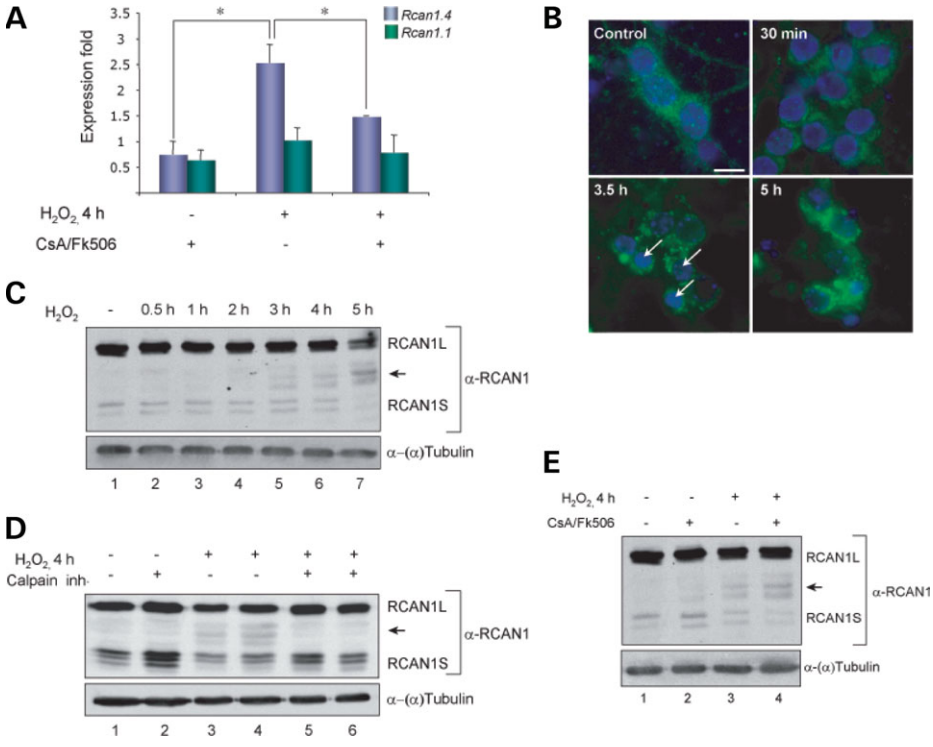

Figure 1. RCAN1 expression after OS. (**A**) *Rcan1.4* and *Rcan1.1* expression after OS. Semi-quantitative real-time PCR was used to determine *Rcan1.1* and *Rcan1.4* mRNA expression relative to *L7* mRNA. All data are expressed relative to basal expression (non-treated cultures), which is assigned a value of 1-fold (1x). Neurons were incubated with CsA (1 μM) and FK506 (0.5 μM) before treatment with 100 μM H_2O_2 for 4 h. Data are presented as the means ± SD of four independent determinations. *, $P < 0.05$. (**B**) RCAN1 immunofluorescence in control granule neurons and at different times after exposure to 50 μM H_2O_2. Abnormal condensed nuclei are already apparent 3.5 h after exposure to H_2O_2 (arrow); scale bar, 10 μM. (**C**) Western blot of RCAN1 protein expression. Neurons were cultured for 7 days and treated for the indicated times with 50 μM H_2O_2. Tubulin expression was used to confirm equal loading. Decreased RCAN1 expression is evident after 5 h. The arrow indicates the progressive appearance of RCAN1 immunoreactive bands around 30 kDa. (**D**) Calpain participates in RCAN1 degradation. Neurons were pretreated with calpain inhibitors I and II (1 μM each) for 20 min before exposure to 50 μM H_2O_2 for 4 h followed by western blotting. (**E**) CaN modulates RCAN1 degradation. Neurons were pretreated of with CsA (1 μM) and FK506 (0.5 μM) for 20 min. Protein samples were extracted for western blot 4 h after the addition of 50 μM H_2O_2.

degradation (Fig. 1E), thus indicating that CaN activity might limit calpain-mediated RCAN1 degradation in response to OS.

Lack of RCAN1 is linked to neuronal susceptibility to OS

To examine the function of RCAN1 in neurons exposed to OS, we used primary neurons cultured from mice with a targeted deletion in the *Rcan1* gene (Fig. 2A). The lack of RCAN1 expression in these cells was confirmed by western blot (Fig. 2B). There were no differences between wild type [$Rcan1^{+/+}$] and knockout [$Rcan1^{-/-}$] neurons in their expression of CaN or of other members of the RCAN family (RCAN2 and RCAN3) (Fig. 2B). Cultures of the two genotypes had similar proportions of granule neurons and astrocytes after 7 to 10 days' culture (data not shown), and the neurons showed similar morphology (Fig. 2C).

The susceptibility of $Rcan1^{+/+}$ and $Rcan1^{-/-}$ neurons to OS-induced damage was determined by MTT assay after 20 h exposure to different doses of H_2O_2. In both genotypes, maximal damage was achieved with 100 μM H_2O_2 (Fig. 3A); however, neurons lacking RCAN1 were more resistant to OS. Calculated IC_{50} values were 55.7 ± 1.6 μM for $Rcan1^{-/-}$ and 46.6 ± 1.1 μM for $Rcan1^{+/+}$ cultures. This result was confirmed by simultaneous staining with fluorescein diacetate (FDA) and propidium iodide (PI) to measure viable and dead cells. Unstimulated $Rcan1^{+/+}$ cultures contained a slightly higher proportion of dead cells compared with unstimulated $Rcan1^{-/-}$ cells (Fig. 3B). This difference was greatly enhanced after exposure to 50 μM H_2O_2, with $Rcan1^{-/-}$ showing a considerable resistance to OS-induced cell death. This relatively higher viability of $Rcan1^{-/-}$ primary neurons was also detected in response to OS induced by the peroxynitrite donor SIN-1 (17% more resistant than $Rcan1^{+/+}$ cultures, $P < 0.05$; data not shown).

We also determined the exposure time to H_2O_2 needed to achieve a maximal detrimental effect (Fig. 3C). $Rcan1^{+/+}$ and $Rcan1^{-/-}$ neurons were exposed to 100 μM H_2O_2 for different periods, and neuronal viability measured 20 h later. Maximal reduction of $Rcan1^{+/+}$ neuronal viability was achieved by exposure to H_2O_2 for 30 min. Again, $Rcan1^{-/-}$ primary neurons were resistant to OS-mediated neuronal death, displaying an increased viability at 30 min and at all shorter exposure times tested.

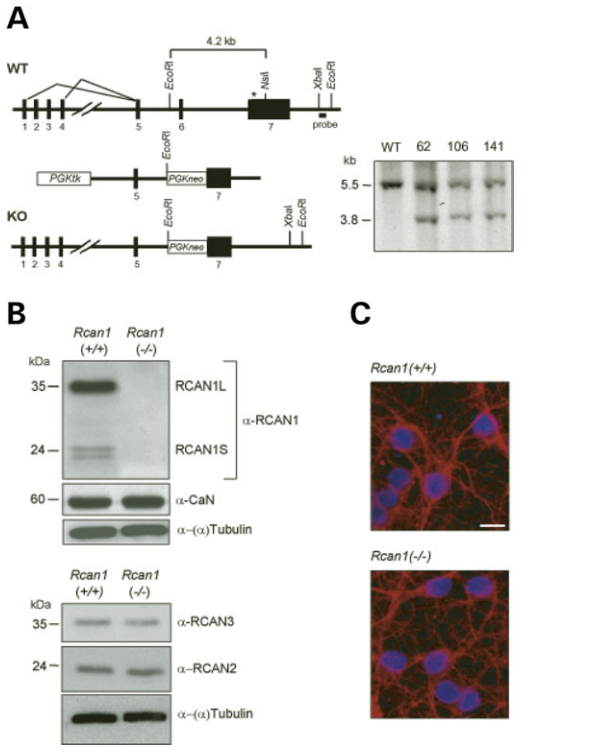

Figure 2. *Rcan*$^{-/-}$ and *Rcan1*$^{+/+}$ granule neurons express similar amounts of CaN and of RCAN-2 and RCAN-3. (**A**) *Left*: schematic diagram showing the genomic structure of the *Rcan1* wild-type (WT) allele, the targeting vector (*Middle*) and the homologous recombinant (KO) allele. Alternative splicing events between exon 1 or 4 and exon 5 are indicated; these events result in *Rcan1.1* and *Rcan1.4* transcripts, respectively. The asterisk shows the location of the STOP codon in exon 7. *Right*: Southern blot of *Eco*RI-digested DNA from the wild-type parental ES cell line and three recombinant clones (clones 62, 106 and 141) hybridized with the *Rcan1* 3'-flanking probe shown in the diagram. (**B**) *Rcan1*$^{-/-}$ and *Rcan1*$^{+/+}$ primary neurons were cultured *in vitro* for 10 days, and analyzed by western blotting for CaN, RCAN1, RCAN2 and RCAN3. (**C**) Immunoflurescence with anti α-tubulin antibody shows that *Rcan1*$^{-/-}$ neurons have no gross abnormalities in cell morphology or neuritic complexity; scale bar 10 μM.

RCAN1 expression in *Rcan*$^{+/+}$ and *Rcan1*$^{-/-}$ primary neurons increases susceptibility to OS

The reduced susceptibility of *Rcan1*$^{-/-}$ neurons to OS is likely the result of the lack of expression of RCAN1 protein. To test this, we attempted to restore the wild type OS response by exogenously expressing RCAN1 in *Rcan1*$^{-/-}$ neurons. To finely control the amount of exogenously expressed RCAN1, we used an adenovirus that expresses both RCAN1S and EGFP (AdRCAN1) (32). Infection with an adenovirus expressing EGFP and firefly luciferase (AdGFPLuc) (33) was used as a control. *Rcan1*$^{-/-}$ neurons transduced with AdRCAN1 at an MOI of 2.5, showed levels of RCAN1S expression comparable to the endogenous expression in wild type controls (Fig. 4A, compare 2 and 3).

The susceptibility to OS of neurons infected with control virus was similar to that of non-infected neurons (Fig. 4B, 4 and 5), thus indicating that infection *per se* did not modify the response to H_2O_2-induced damage. In contrast, the incidence of H_2O_2-mediated death was increased in *Rcan1*$^{+/+}$ and *Rcan1*$^{-/-}$ primary neurons infected with AdRCAN1 (Fig. 4B, 3). Furthermore, the sensitivity to H_2O_2 of *Rcan1*$^{-/-}$ neurons overexpressing RCAN1 was similar to that of non-infected *Rcan1*$^{+/+}$ neurons (Fig. 4B, compare 3 with 5). These data thus indicate that the level of RCAN1 protein is directly responsible for the differential response of *Rcan1*$^{+/+}$ and *Rcan1*$^{-/-}$ to ROS-mediated damage.

H_2O_2-induced Ca^{2+} uptake is similar in *Rcan1*$^{+/+}$ and *Rcan1*$^{-/-}$ neurons

Redox status-dependent cation channels have been shown to underlie susceptibility to OS-mediated death by inducing Ca^{2+} overloading (34,35). We therefore determined H_2O_2-induced changes in Ca^{2+} homeostasis in *Rcan1*$^{+/+}$ and *Rcan1*$^{-/-}$ neurons loaded with the Ca^{2+} indicator Fluo-3, to see if this could account for the different sensitivities of these cells to H_2O_2 (Fig. 5). Exposure of neurons to 100 or 250 μM H_2O_2 progressively increased the intracellular Ca^{2+} concentration in both genotypes, with no significant differences detected (Fig. 5A). Mean Ca^{2+} responses of *Rcan1*$^{+/+}$ and *Rcan1*$^{-/-}$ cultures were not significantly different, whether the cells were unstimulated (fluorescence ratio $= 1.06 \pm 0.08$, $n = 132$ neurons *versus* 1.05 ± 0.02, $n = 127$ neurons) or stimulated with 250 μM H_2O_2 (2.18 ± 0.06, $n = 170$ *versus* 1.98 ± 0.06, $n = 157$) ($P > 0.05$). Identical patterns were observed with higher H_2O_2 concentrations, although the magnitude of Ca^{2+} signals was larger and the response latency shorter (data not shown). Figure 5B shows individual fluo-3 images obtained from granule neurons treated with 250 μM H_2O_2 in a Ca^{2+}-free solution. Under these conditions, no increases in Ca^{2+} were observed either in *Rcan1*$^{+/+}$ or in *Rcan1*$^{-/-}$ cultures. However, both neuron genotypes showed an acute rise in intracellular Ca^{2+} upon exposure to a Ca^{2+}-containing solution. Thus, most of the H_2O_2-induced rise in Ca^{2+} has an extracellular origin, which suggests the presence of Ca^{2+} channels sensitive to OS. The channels most likely to account for OS-induced Ca^{2+} entry belong to the TRP family, with the TRPM2 channel a particularly strong candidate (35,36).

Pre-incubation with 10 μM gadolinium (Gd^{3+}), a non-selective blocker of TRP channels, reduced the Ca^{2+} increase by 60–70% (Fig. 5C); and Gd^{3+} also reduced H_2O_2-induced cell death (Fig. 5D), suggesting that Ca^{2+} influx is in part responsible for neuronal death. Pre-incubation with the antioxidant agent Trolox (a vitamin-E analogue) blocked the H_2O_2-induced Ca^{2+} increase (data not shown). These data indicate that the initial Ca^{2+} increase following exposure to H_2O_2 is dependent on extracellular Ca^{2+} and ROS both in wild type and in *Rcan1*-deficient neurons. The similar perturbation of calcium homeostasis by H_2O_2 in the two genotypes indicates that their differential susceptibility to OS is likely to involve a mechanism downstream of Ca^{2+} entry.

CaN and NFAT signaling pathways limit H_2O_2-induced death in *Rcan1*$^{+/+}$ and *Rcan1*$^{-/-}$ neurons

The principal molecular target described for RCAN1 is the phosphatase CaN. We therefore evaluated the possible

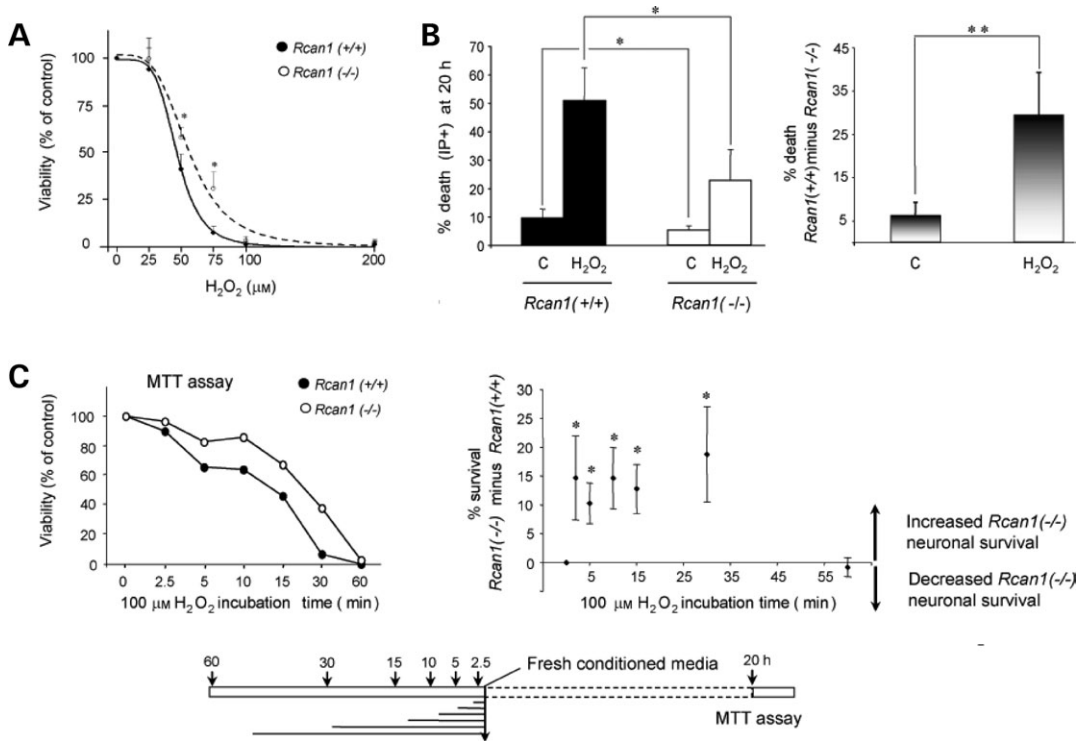

Figure 3. *Rcan1*$^{-/-}$ neurons have increased resistance to H_2O_2 induced stress. (**A**) Dose response to H_2O_2-mediated damage. Neurons were cultured *in vitro* for 7–10 days and chronically treated with the indicated concentrations of H_2O_2. Cell viability was determined 20 h later by MTT assay in triplicate for each condition and cell culture. Values are expressed as the percentage of the viability of control neurons not subjected to OS, which was assigned the value of 100%. Data are presented as the mean ± SD of determinations performed in four independent paired *Rcan1*$^{+/+}$ and *Rcan1*$^{-/-}$ neuronal cultures. *, $P < 0.05$. (**B**) Neuronal death induced by chronic exposure to 50 μM H_2O_2. The left panel shows the proportion of dead (PI-positive) cells for each genotype and condition, calculated as a percentage of the total number of cells (PI-positive plus FDA-positive). For the right panel, the percentage of dead cells in *Rcan1*$^{-/-}$ cultures was subtracted from that obtained the parallel-treated *Rcan1*$^{+/+}$ cultures. Data are presented as the mean ± SD of determinations performed in five independent paired *Rcan1*$^{+/+}$ and *Rcan1*$^{-/-}$ neuronal cultures.*, $P < 0.05$; **, $P < 0.001$. (**C**) Viability of *Rcan1*$^{-/-}$ and *Rcan1*$^{+/+}$ neurons as a function of the exposure time to 100 μM H_2O_2. Paired *Rcan1*$^{-/-}$ and *Rcan1*$^{+/+}$ neuronal cultures were simultaneously exposed to H_2O_2, and culture media were removed and replaced with fresh conditioned media at the indicated times. Cell viability was determined by MTT assay after 20 h. The left panel shows a representative plot of four independent determinations. For the right panel, *Rcan1*$^{+/+}$ viability was subtracted from *Rcan1*$^{-/-}$ viability for each independent determination and exposure time. The positive values obtained indicate an increased resistance of *Rcan1*$^{-/-}$ neurons to H_2O_2-mediated damage. Data are the mean ± SD of cell viability values of *Rcan1*$^{-/-}$ minus *Rcan1*$^{+/+}$ *, $P < 0.05$.

involvement of CaN in OS-induced neuronal death by pretreating *Rcan1*$^{+/+}$ and *Rcan1*$^{-/-}$ primary neurons with a combination of the CaN inhibitors CsA and FK506, followed by acute (15 min) exposure to 100 μM H_2O_2 (Fig. 6A). CsA and FK506 did not affect neuronal survival under basal conditions, but the inhibitors significantly enhanced neuronal death induced by H_2O_2. These data suggest that, while CaN signaling is dispensable for cell viability under basal culture conditions over the time-course examined, its activity is protective following H_2O_2-induced stress. The extent of H_2O_2-mediated cell death in *Rcan1*$^{-/-}$ neurons pretreated with CsA/FK506 was similar to that detected in non-pretreated *Rcan1*$^{+/+}$ neurons (Fig. 6A), which suggests that CaN is involved in the genotype-related differential susceptibility to OS.

One of the best-characterized signaling pathways regulated by CaN involves the activity of the nuclear factor of activated T cells (NFAT) family of transcription factors. Dephosphorylation of NFAT proteins by CaN is required for their nuclear import and subsequent transcriptional activity (37,38). Our results showing a specific H_2O_2-dependent induction of *Rcan1.4* (Fig. 1A) strongly suggest that NFAT signaling is activated after OS, which is in agreement with ROS-mediated NFAT activation in other cell types (39,40). Furthermore, recent data have shown the participation of NFAT signaling in cerebellar granule neuron survival (41). We used the VIVIT peptide to assess the possible involvement of NFAT signaling in OS-induced neuronal damage. VIVIT specifically inhibits NFAT-dependent transcription through its ability to block the interaction between CaN and NFAT without affecting CaN activity (42). *Rcan1*$^{+/+}$ and *Rcan1*$^{-/-}$ primary neurons were transfected with GFP-VIVIT or GFP expression vectors and the proportion of transfected cells showing nuclear PI staining was determined (Fig. 6B). Under resting conditions, VIVIT overexpression had no significant effect on neuronal viability. However, VIVIT-expressing neurons were appreciably more sensitive to H_2O_2 (Fig. 6B), suggesting that NFAT activity has a neuroprotective effect in the response to OS. These data support a model in which the differential sensitivity of wild type and RCAN1-deficient neurons to OS is mediated by CaN signaling through a mechanism involving NFAT transcriptional activity.

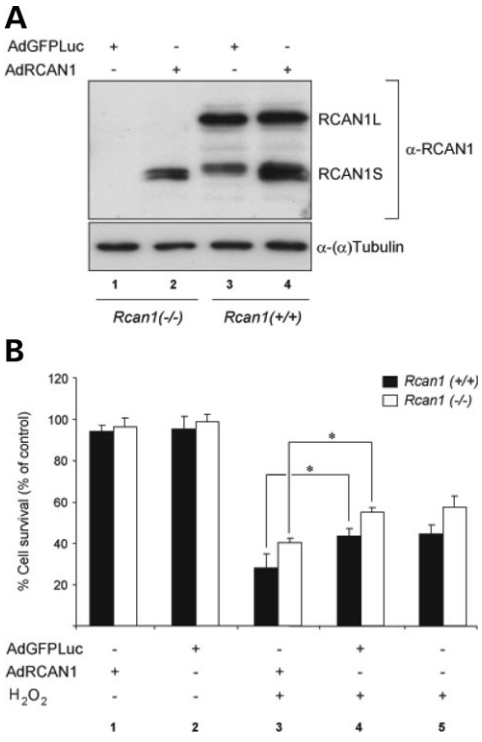

Figure 4. RCAN1 overexpression increases neuronal susceptibility to OS. (**A**) Western blot of RCAN1 protein expression. Parallel *Rcan1*$^{+/+}$ and *Rcan1*$^{-/-}$ primary neuronal cultures were cultured for 2 days (DIV 2) and simultaneously transduced with AdGFPLuc and AdRCAN1, MOI = 2.5. RCAN1 expression was analyzed 4 days later. (**B**) Parallel *Rcan1*$^{+/+}$ and *Rcan1*$^{-/-}$ primary neurons were cultured for 2 days and simultaneously transduced with AdRCAN1 (1 and 3) or AdGFPLuc (2 and 4) at MOI = 2.5. 4 days later, cultures were treated with 50 μM H_2O_2 (3, 4 and 5), and cell viability was determined by MTT assay, 6 h later in three independent wells per condition. Data are presented as the mean ± SD of determinations in three independent experiments *, $P < 0.05$.

DISCUSSION

In this study, we have described the expression pattern of the endogenous CaN modulator RCAN1 in response to OS, and have shown that RCAN1 is a detrimental factor in this response, contributing to ROS-mediated damage.

Our analysis of the expression pattern of RCAN1 after OS in primary granule neurons shows that H_2O_2-mediated *Rcan1.4* induction is not associated with a concomitant increase in RCAN1S protein levels, which is in accordance with previous results on human non-neuronal cell lines submitted to OS (27,28). These data suggest that processes that regulate RCAN1 translation and/or stability might influence the final expression output. Supporting this, we detected calpain-dependent RCAN1 degradation after exposure to H_2O_2. Since RCAN1 degradation is detected at 4–5 h after OS, our results indicate that *Rcan1.4* mRNA induction at 4 h after treatment may not be relevant in maintaining RCAN1S levels. These degradation products might not have full RCAN1 functionality since *in vitro* cleavage of RCAN1 produces fragments with reduced affinity for CaN (30). Our results further indicate that after OS CaN is able to modulate RCAN1 expression at different levels, inducing *Rcan1.4* mRNA expression and limiting RCAN1 cleavage by calpain. Thus, RCAN1 expression and functionality might depend, at least in part, on the timing and relative strengths of these two processes. Our results contrast with previous reports showing that RCAN1L and RCAN1S become hyperphosphorylated shortly after exposure to H_2O_2, as indicated by changes in the proportion of the RCAN1 protein bands with different electrophoretic mobilities (27,28). However, these studies used non-neuronal cell lines, and no cell damage was reported even though cells were treated with high H_2O_2 concentrations (500 μM). The increased resistance to OS of these cell lines compared with primary neurons might reflect differences in intracellular signaling pathways, which in turn, could explain the lack of RCAN1 post-translational modifications in neurons. Nevertheless, OS-linked changes to the pattern of RCAN1 phosphorylation should be considered in every cell type analyzed, since RCAN1 phosphorylation status is relevant to its function as a modulator of CaN (10,43,44). Another feature of the RCAN1 expression pattern after OS is the shift in its cytoplasmic appearance to the form of coarse granules. The exact nature of these structures and their relevance to the neuronal response to OS remain to be elucidated. However, since OS leads to protein aggregation (45) and recent studies have shown that RCAN1 contains an aggregation-prone domain at the N-terminal region (21), it could be hypothesized that these granules correspond to ROS-mediated aggregates of RCAN1.

Our data indicate that CaN is activated after exposure to H_2O_2, since exogenous CaN inhibitors alter not only RCAN1 mRNA expression, but also neuronal susceptibility to ROS-mediated damage. Similarly, H_2O_2-dependent activation of CaN has been shown in cerebellar granule neurons (29) and in hippocampal slices (46). The increased OS-induced damage we detected in the presence of exogenous CaN inhibitors suggests that this phosphatase protects against H_2O_2 toxicity in primary cerebellar neurons. Studies conducted in different cell types have demonstrated either pro- or antiapoptotic effects associated with CaN activation. For instance, there is considerable evidence suggesting that CaN activity contributes to neuronal apoptosis associated with glutamate excitotoxicity and ionophore-induced Ca^{2+} overloading (47–50). In other systems, such as cultured cardiac myocytes, CaN activation protects against H_2O_2- or 2-deoxyglucose- induced death (51,52). In agreement with this, CaNAβ-deficient mice have an elevated susceptibility to cardiac damage (53). Collectively, these accounts underscore the complexity of intracellular signaling networks within mammalian cells, with seemingly related stress stimuli able to elicit fundamentally different responses.

A key finding of our study is that blockade of NFAT activity increases neuronal susceptibility to ROS-induced damage. Therefore, the protective role of CaN activity in the response to OS might be mediated, at least in part, by NFAT transcriptional activity. On the other hand, a previous study has shown that oxidative damage in granule neurons is partially due to CaN-mediated dephosphorylation of the transcription factor CREB (29). Thus, OS-mediated CaN activation might trigger prosurvival and detrimental signals. The strength and duration of the stimulated pathways may determine the overall effect on neural viability.

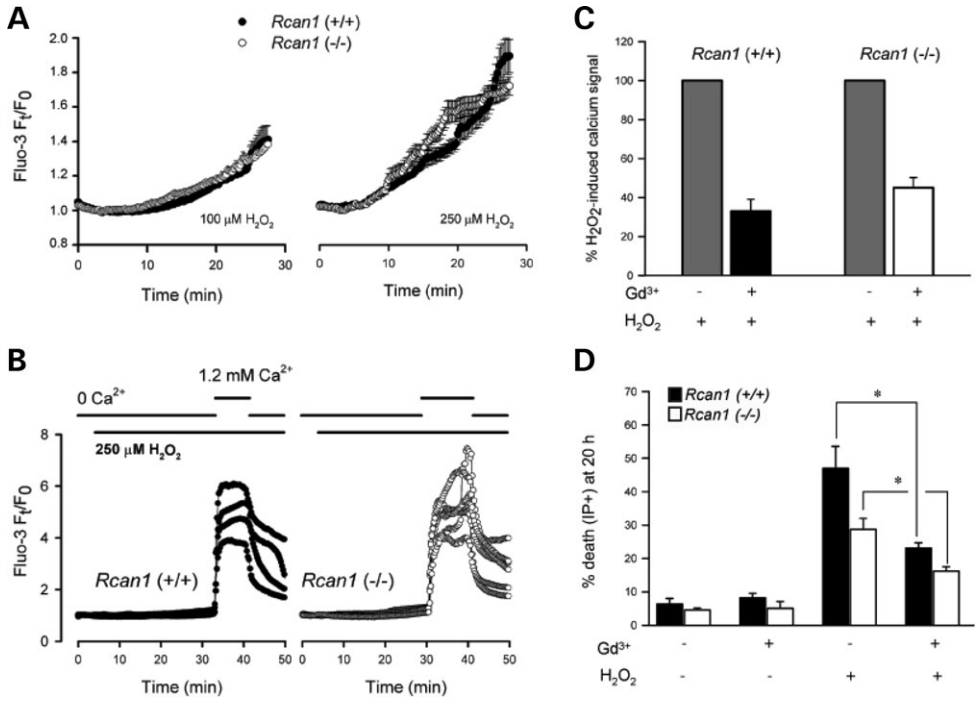

Figure 5. H_2O_2-induced $[Ca^{2+}]_i$ changes in individual neurons. (**A**) *Rcan1*$^{+/+}$ (black circles) and *Rcan1*$^{-/-}$ (white circles) neurons were exposed in parallel to 100 μM or 250 μM H_2O_2 at time = 3 min. Plots show mean ± S.E.M. of responses obtained from 20 to 30 neurons. (**B**) After 30 min in Ca^{2+}-free solution containing 250 μM H_2O_2, cells were briefly exposed to 1.2 mM Ca^{2+}, as indicated. (**C**) Gd^{3+} inhibits Ca^{2+} entry induced by 250 μM H_2O_2. Gd^{3+} (10 μM) was added at time=0 in the protocol shown in A. (**D**) Gd^{3+} reduces HO_2-mediated neuronal death. Neurons were pretreated (20 min) with 10 μM Gd^{3+}; and exposed to 50 μM H_2O_2 for 20 h. Neuronal death was determined by FDA and PI fluorescent double staining; $P < 0.05$, $n = 4$.

The role of RCAN1 in ROS-mediated damage was evaluated in this study with a mouse model of RCAN1 deficiency. The increased resistance of RCAN1-deficient neurons indicates that this protein is detrimental to cell survival after OS. Paradoxically, ROS-mediated degradation of extant RCAN1 protein was apparent 4–5 h after exposure to H_2O_2, which would suggest that RCAN1 might be protective against OS. However, our data indicate that degradation of RCAN1 begins after OS-mediated neuronal damage is already underway (Fig. 1B), and therefore after the detrimental role of RCAN1 in the neuronal susceptibility to OS is likely to have taken place. Furthermore, the possible harmful action of the RCAN1 degradation products, further contributing to cell death, cannot be discarded. The greater resistance of *Rcan1*$^{-/-}$ primary neurons to OS agrees with the notion that RCAN1 acts as a negative modulator of CaN in this experimental model. An increased CaN response in the *Rcan1*$^{-/-}$ neurons is suggested by the rescue of the wild type susceptibility to OS with CsA/FK506. However, RCAN1 has been recently described as a facilitator of CaN activity in the brain, since *Rcan1* −/−, *CaNB1* −/− and *CaNA*β −/− mice showed a similar phenotype of hyperactivity and working memory deficit (54). Considered together, these findings suggest that RCAN1 can facilitate or suppress CaN signaling in neurons depending on the nature of the stimulus and the status of other parallel signaling pathways.

Regarding the molecular mechanisms underlying differential susceptibility, our data indicate that although initial Ca^{2+} overloading plays an important role in ROS-mediated neuronal death, neither the kinetics nor the amount of Ca^{2+} entry were modified in *Rcan1*$^{-/-}$ neurons. An explanation for the increased resistance of RCAN1-deficient neurons could be that RCAN1 normally limits CaN-mediated prosurvival actions after OS. In this way RCAN1 would forestall certain CaN-mediated prosurvival effects, including those mediated by the CaN-NFAT signaling pathway. In this scenario, the lack of RCAN1 would be expected to increase beneficial actions of CaN, specifically those linked to OS. It has recently been proposed that the ability of RCAN1 to modulate the pattern of CaN-dependent transcription depends on the transactivation thresholds of the NFAT target genes (55). This scheme fits with the contrast we observed between the mild effect of RCAN1 deficiency on neuronal viability under resting conditions and the significantly reduced incidence of neuronal death in response to OS. Therefore, it is feasible that RCAN1 has a discriminating action, permitting the expression of CaN-dependent prosurvival genes under resting conditions, but limiting their expression after OS. In apparent contradiction, a positive correlation has been shown between RCAN1 dose and protection from OS in the PC12 neural cell line (19). In that report, however, the readouts of H_2O_2-mediated stress were colony forming ability and cell growth, using a method that corrects for cell death due to ROS-mediated toxicity (56). Thus although one cannot rule out an opposite effect of RCAN1 dose on cell viability in primary neurons and PC12 cells, it may simply be that the experimental approaches used are not comparable.

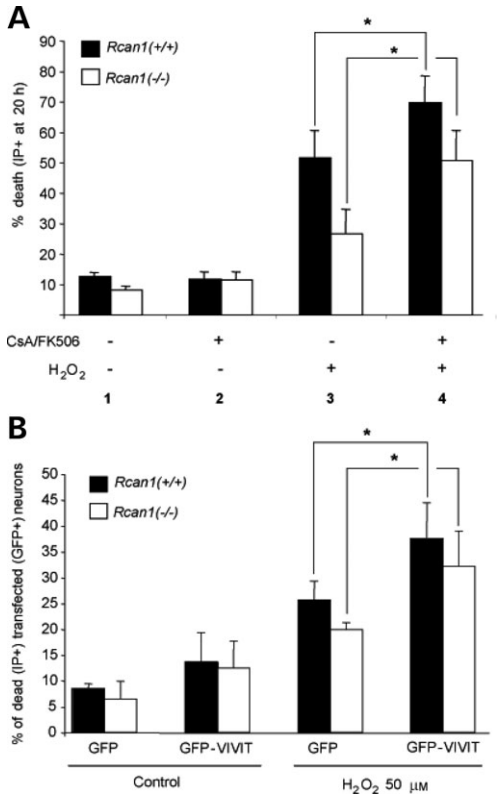

Figure 6. CaN and NFAT signaling modulate the neuronal response to OS both in *Rcan1*$^{+/+}$ and in *Rcan1*$^{-/-}$ neurons. (**A**) CaN activity modulates neuronal susceptibility to OS. Neuron cultures were pretreated with CsA (1 μM) and FK506 (0.5 μM) and exposed to 100 μM H_2O_2 for 15 min. H_2O_2 was then washed out and conditioned culture medium containing CsA/FK506 added. Neuronal damage was determined 20 h later, using the FDA + PI double-staining method. The incidence of neuronal death was calculated as in Figure 3B. Notice increased sensitivity to H_2O_2 upon CaN inhibition. Data are presented as the mean ± SD of parallel determinations in five independent paired *Rcan1*$^{+/+}$ and *Rcan1*$^{-/-}$ neuronal cultures. *, $P < 0.05$. (**B**) NFAT signaling participates in the *Rcan1*$^{+/+}$ and *Rcan1*$^{-/-}$ neuronal response to OS. Granule neurons were transfected with VIVIT-GFP or GFP and chronically treated with 50 μM H_2O_2. The number of GFP positive cells with PI-positive nuclei was determined 16 h later and plotted as a percentage of the total number of GFP positive cells. Data are presented as the mean ± SD of four independent pairs of transfected *Rcan1*$^{+/+}$ and *Rcan1*$^{-/-}$ cultures. *, $P < 0.05$.

Another key finding is that neuronal sensitivity to OS was increased by RCAN1 overexpression. Since OS has been associated with DS and AD, it is reasonable to hypothesize that overexpressed RCAN1 contributes to neuronal dysfunction in these neurological disorders. In summary, the results we have presented establish the importance of RCAN1 dosage in the neuronal response to OS and further highlight that processes modulating RCAN1 expression and dosage could represent new therapeutic targets in the context of neurodegenerative processes.

MATERIALS AND METHODS

Gene targeting and generation of *Rcan1*$^{-/-}$ mice

To construct the targeting vector, genomic sequences of the mouse strain 129SVJ were obtained from a Lambda library (Stratagene) and subcloned into pGem-7Zf(+) (Promega). A 4.2 kb *Rcan1* genomic fragment was then replaced by the *PGKneobpA* cassette. A *PGKtk* cassette was added at the 5'-arm of the homology sequences for negative selection (Fig. 2A). The resulting construct was linearized and electroporated into the 129OlaHsd ES cell line (E14-1) as described previously (57). Clones resistant to G418 and gancyclovir were selected for homologous recombination by Southern blotting using *EcoRI*-digested DNA and a 3'-flanking probe (Fig. 2A). Bona fide recombinant clones were microinjected into C57BL/6 blastocysts resulting in male chimeras that were subsequently bred with C57BL/6 females to produce heterozygous *Rcan1*(+/−) offspring.

In this work, we used the progeny of wild-type *Rcan1*$^{+/+}$ and knockout *Rcan1*$^{-/-}$ mice obtained after backcrossing *Rcan1*$^{+/-}$ mice of the F1 generation with C57BL/6 mice. Animals were genotyped by Southern blotting or PCR analysis using genomic DNA from tail biopsies. PCR oligonucleotide primers used were the following: *neo*-T (5'-ATTCGCAGCG CATCGCCTTCTATCGCC-3'), *Rcan1*-R8 (5'-GGTGGTCC ACGTGTGTGAGA-3'), and *Rcan1*-R15 (5'-ACGTGAACA AAGGCTGGTCCT-3').

Animals were housed in the CRG-IMIM animal facility, and were reared and sacrificed in accordance with recommendations and protocols approved by the local Ethics Committee.

Neuronal cell culture and treatments

Primary cultures of mouse cerebellar granule neurons were prepared as previously reported (58) with some modifications. In brief, cerebella from 7-day-old mouse pups were isolated, cut into small pieces and then trypsinized at 37°C. To ensure comparability of results between genotypes and to minimize experimental variability, *Rcan1*$^{+/+}$ and *Rcan1*$^{-/-}$ neurons were established and treated in parallel. Dissociated cells were seeded at 5×10^5 cells/cm^2 into poly-lysine-coated culture dishes, and were grown at 37ºC in a humidified 5% CO_2 atmosphere in DMEM (Gibco) supplemented with 10% FCS (DMEM–FCS) containing 25 μM KCl. After 24 h, medium was replaced with a 1:1 mixture of DMEM–FCS and Neurobasal™ medium (Gibco) containing B-27 (Gibco) and 25 mM KCl (Neurobasal™/B27) supplemented with cytosine arabinoside (Ara-C, 10 μM final concentration) (Sigma). Neurons were then cultured for an additional 7 to 10 days (DIV-7-DIV10) before treatments.

H_2O_2 solutions were freshly prepared from a 30% H_2O_2 stock solution (Merck). Neuronal cultures were exposed to the indicated concentrations of H_2O_2 either chronically or acutely (15 min). Chronic exposure to 50 μM H_2O_2 and acute treatment with 100 μM H_2O_2 were similarly toxic. In acute treatments, medium containing H_2O_2 was removed after 15 min, and replaced with conditioned medium. FK506, CsA and calpain inhibitors I and II (Calbiochem) were added 20 min before exposure to H_2O_2, and were maintained throughout the experiment.

Western blot analysis

Cell homogenates were prepared from primary neurons plated in 24 well plates by rinsing with phosphate buffered saline

(PBS) and lysing with 80 μl/well of SDS-sample buffer. Samples were collected and immediately heated for 5 min at 100°C. Proteins were resolved by 12% SDS–PAGE, and electroblotted onto nitrocellulose membranes (Hybond-C extra, Amersham Life Sciences). Membranes were blocked with 10% skimmed milk in TBS buffer (0.1% Tween-20, 140 mM NaCl and 10 mM Tris–HCl, pH 7.4) followed by incubation in 5% skimmed milk in TBS buffer with the primary antibody overnight at 4°C. Antibodies against the different members of the RCAN family were generated in our lab, using the synthetic peptides RPEYTPIHLS, RPGLPPSVSN or ALSERLDCAL, which are respectively located in the carboxy-terminal regions of mouse RCAN1, RCAN2 (also named CALP2) and RCAN3 (also named CALP3). The resultant affinity-purified antibodies were highly specific and showed no cross-reactivity among the different members of the RCAN family (S. Porta, unpublished data). Anti-RCAN1, anti-RCAN2 and anti-RCAN3 were used at dilutions of 1:1000 and 1:2000 and 1:100, respectively. The monoclonal antibodies to calcineurin (Pharmigen, BD) and α-tubulin (Sigma) were used at dilutions of 1:500 and 1:10 000, respectively. After incubation with primary antibody, membranes were washed in TBS buffer, and incubated for 1 h at room temperature with peroxidase-conjugated anti-mouse or anti-rabbit (Dako) secondary antibodies at a dilution of 1:2000. After washing, membranes were developed with the enhanced chemiluminiscence system (ECL, Amersham Life Sciences).

Immunofluorescence

Primary cell cultures grown on coverslides were rinsed several times with PBS and fixed for 20 min at room temperature with 4% paraformaldehyde in PBS. After rinsing, cells were permeabilized for 20 min in 0.5% Triton-X-100 in PBS. Nonspecific binding sites were then blocked by incubating for 1 h in PBS containing 0.2% Triton X-100 and 10% FBS. Incubation with primary anti-RCAN1 antibody was carried out overnight at 4°C in PBS containing 0.2% Triton-X-100 and 1% FBS. After washing, coverslides were incubated with secondary anti-rabbit IgG antibodies (Molecular Probes) at a dilution of 1:200 for 1 h at room temperature. After washing, coverslides were mounted in Vectashield-DAPI solution, and cells visualized under a Leica microscope (DMR). Images were captured using a digital camera (Leica DC500).

Semiquantitative RT–PCR

RNA was isolated from primary neuronal cell cultures using the Rneasy kit (Qiagen). After treatment with DNase (Ambion), cDNA was synthesized using 1 μg of total RNA, Superscript II reverse transcriptase (Invitrogen) and random hexamers (Roche). *Rcan1* spliced transcripts were amplified in independent reactions using, respectively, the following forward and reverse sets of PCR primers: *Rcan1*-e1 (5'-ccgtagggtgactctg-3') and *Rcan1*-e5a (5'-gctcttaaaatactgg aaggt-3') for *Rcan1.1*; and *Rcan1*-e4 (5'-gcgagtcgttcgttaag-3') and *Rcan1*-e5b (5'-atactggaaggtggtgt-3') for *Rcan1.4*. To normalize gene expression levels, the following primers specific to ribosomal protein L7 (*L7*) cDNA were used: 5'-gaagctcatctatgagaaggc-3' and 5'-aagacgaaggagctgcagaac-3'. Semi-quantitative real-time PCR was performed using Fast Start DNA Master^{PLUS} SYBR Green I kit (Roche) and a Roche Light Cycler. To compare the abundance of *Rcan1.1* and *Rcan1.4* transcripts in resting cells or after H_2O_2 treatment, their expression was calculated relative to that of L7 transcripts (59).

Colorimetric MTT assay to determine neuronal viability

Cells were cultured in 96-well culture dishes (Culteck) and treated as indicated. Following treatment, mitochondrial activity was assayed with MTT [3-(4,5-dimethylthiazol-2-yl)-2,5-diphenyltetrazolium bromide; Sigma]. Briefly, cultures were incubated for 20 min (37°C) with freshly prepared culture medium containing 0.5 mg/ml MTT. After aspiration of the medium, the dark blue crystals formed were dissolved by adding 100 μl/well of DMSO. Absorbance readings at reference wavelengths of 570 and 630 nm were taken using a Versa max micro plate reader.

Nuclear staining and dye-exclusion assays to determine neuronal death

Cell death was determined with the FDA/PI double staining procedure. Cells were incubated for 45 s at 22–25°C with 15 μg/ml FDA (Sigma) and 4.6 μg/ml PI (Molecular Probes, Inc., Eugene, OR, USA) in PBS. The stained cells were immediately examined under a Leica microscope. A blinded observer counted the number of dead (PI stained) and living (FDA stained) neurons in three microscopic fields (40 × magnification) for each coverslide. The values presented are the means of counts from two coverslides per condition, totaling ~600–800 cells.

Calcium measurements

$[Ca^{2+}]_i$ was monitored in primary granular cells with the fluorescent Ca^{2+} indicator fluo 3-AM. Cells were loaded in a standard bath solution composed of 140 mM NaCl, 2.5 mM KCl, 1.2 mM $CaCl_2$, 0.5 mM $MgCl_2$, 5 mM glucose and 10 mM Hepes (pH 7.25 with Tris-NaOH), supplemented with 5 μM fluo 3-AM (Molecular Probes, Leiden, The Netherlands) and 0.005% Pluronic F-127 (Molecular Probes). Cells were then washed thoroughly with isotonic solution for 15 min. When indicated, Ca^{2+} free bathing solution composed of 140 mM NaCl, 2.5 mM KCl, 1 mM EGTA, 1.5 mM $MgCl_2$, 5 mM glucose and 10 mM Hepes (pH 7.25 with Tris-NaOH) was used.

Video microscopic measurements of Ca^{2+} were obtained with an Olympus IX70 inverted microscope (Hamburg, Germany) fitted with a 40 × oil-immersion objective (Olympus, Hamburg, Germany). The excitation light (489 nm) was supplied by a Polychrome IV monochromator (Till Photonics, Martinsried, Germany) and directed toward the cells under study by a 505DR dichromatic mirror (Omega Optical, Brattleboro, USA). Fluorescence images were first passed through a 535DF emission filter (Omega Optical) and then collected by a digital CCD camera linked to the AquaCosmos software program (Hamamatsu Photonics, Japan). Images were

computed every 10 sec and graphs were normalized to the basal fluorescence signal prior to the addition of H_2O_2.

Transfection and treatments

The GFP-VIVIT construct encodes an N-terminal fusion of the high affinity CaN-binding peptide (VIVIT) to GFP protein, as described previously (42). At day 1 after plating, neurons were transfected using Lipofectamine2000™ according to the instructions provided. A ratio of 1 μg of DNA and 2.5 μl of Lipofectamine2000™ was used per well in a 24 well plate. Two days after transfection, neurons were treated with 50 μM H_2O_2. Neuronal death was determined 20 h later by determining the proportion of transfected neurons (GFP positive) with nuclei stained with PI. Data were obtained from at least four independent transfected cell cultures. A total of 300 neurons were counted per condition.

Adenoviral transduction

Recombinant adenoviral vectors expressing RCAN1 and EGFP (Ad-RCAN1) or Firefly Luciferase and EGFP (Ad-GFPLuc) were propagated in the HEK293 cell line and purified by Caesium Chloride banding according to standard procedures (60). At DIV 3–5, media were removed from neuronal cultures. Purified virus, diluted in 50 μl of Neurobasal™/B27, was added to each well, and cells were incubated for 3 h at 37°C. The virus solution was removed and replaced by an equal mix of conditioned medium and fresh Neurobasal™/B27. Four days after transduction, neuronal cultures were subjected to OS and cell viability was determined by the MTT assay, 4 to 6 h later in three independent wells per condition.

Statistical analysis

Descriptive statistical analysis was performed with SPSS software (SYSTAT software, Inc, Chicago, IL, USA). The Mann–Whitney non-parametric test was used for the statistical analysis (two-tailed) of the neuronal death and survival assays in transfection experiments and transduction studies; $P \leqslant 0.05$ was considered statistically significant. IC_{50} values were estimated from H_2O_2 dose-response curves using a non-linear model (61), and *Rcan1*$^{+/+}$ and *Rcan1*$^{-/-}$ were compared with a permutation test (62); $P \leqslant 0.05$ was considered statistically significant. In the analysis of H_2O_2-induced Ca^{2+} loading, ANOVA and Bonferroni's tests were used for *post hoc* comparison of means. The criterion for a significant difference was $P < 0.05$.

ACKNOWLEDGEMENTS

We thank Dr J. Aramburu for the VIVIT-GFP expression construct, Dr T. Minami for the AdRCAN1 adenovirus, Drs S. de la Luna and C. Fillat for discussion and comments on the manuscript, Dr J.R. González for the stadistical analysis, and Dr S. Bartlett for linguistic help. We also thank the staff of the IMIM animal facility and to N. Berbel and E. Ramírez for animal care. Financial Support was received from the Spanish Ministry of Health 'Fondo de Investigaciones Sanitarias -FIS-' (CIBER-CB06/02/0058, CIBER-CB06/07/0089, red HERACLES), the Spanish Ministry of Education and Science (grant numbers SAF2003–1240, SAF2004–01821 and SAF2006–4793), and the Generalitat de Catalunya (SGR05–266) and the Department of Universities, Research and Information Society (2005SGR00008). S. Porta is supported by the CRG under the EU project QLG1_CT-2002–00816; M. Huch by the Spanish Ministry of Health (BEFI predoctoral fellowship); F. Llorens by the Spanish Ministry of Education and Science (Juan de la Cierva Program) and E. Martí by the CRG and the Spanish Ministry of Health (FIS).

Conflict of Interest statement. The authors wish to declare no competing financial interests.

REFERENCES

1. Kingsbury, T.J. and Cunningham, K.W. (2000) A conserved family of calcineurin regulators. *Genes Dev.*, **14**, 1595–1604.
2. Fuentes, J.J., Genescà, L., Kingsbury, T.J., Cunningham, K.W., Perez-Riba, M., Estivill, X. and de la Luna, S. (2000) DSCR1, overexpressed in Down syndrome, is an inhibitor of calcineurin-mediated signaling pathways. *Hum. Mol. Genet.*, **9**, 1681–1690.
3. Rothermel, B., Vega, R.B., Yang, J., Wu, H., Bassel-Duby, R. and Williams, R.S. (2000) A protein encoded within the Down syndrome critical region is enriched in striated muscles and inhibits calcineurin signaling. *J. Biol. Chem.*, **275**, 8719–8725.
4. Rothermel, B.A., Vega, R.B. and Williams, R.S. (2003) The role of modulatory calcineurin-interacting proteins in calcineurin signaling. *Trends Cardiovasc. Med.*, **13**, 15–21.
5. Shibasaki, F., Hallin, U. and Uchino, H. (2002) Calcineurin as a multifunctional regulator. *J. Biochem. (Tokyo)*, **131**, 1–15.
6. Fuentes, J.J., Pritchard, M.A., Planas, A.M., Bosch, A., Ferrer, I. and Estivill, X. (1995) A new human gene from the Down syndrome critical region encodes a proline-rich protein highly expressed in fetal brain and heart. *Hum. Mol. Genet.*, **4**, 1935–1944.
7. Fuentes, J.J., Pritchard, M.A. and Estivill, X. (1997) Genomic organization, alternative splicing, and expression patterns of the DSCR1 (Down syndrome candidate region 1) gene. *Genomics*, **44**, 358–361.
8. Casas, C., Martinez, S., Pritchard, M.A., Fuentes, J.J., Nadal, M., Guimera, J., Arbones, M., Florez, J., Soriano, E., Estivill, X. *et al*. (2001) Dscr1, a novel endogenous inhibitor of calcineurin signaling, is expressed in the primitive ventricle of the heart and during neurogenesis. *Mech. Dev.*, **101**, 289–292.
9. Yang, J., Rothermel, B., Vega, R.B., Frey, N., McKinsey, T.A., Olson, E.N., Bassel-Duby, R. and Williams, R.S. (2000) Independent signals control expression of the calcineurin inhibitory proteins MCIP1 and MCIP2 in striated muscles. *Circ. Res.*, **87**, E61–E68.
10. Genescà, L., Aubareda, A., Fuentes, J.J., Estivill, X., de La Luna, S. and Perez-Riba, M. (2003) Phosphorylation of calcipressin 1 increases its ability to inhibit calcineurin and decreases calcipressin half-life. *Biochem. J.*, **374**, 567–575.
11. U, M., Shen, L., Oshida, T., Miyauchi, J., Yamada, M. and Miyashita, T. (2004) Identification of novel direct transcriptional targets of glucocorticoid receptor. *Leukemia*, **18**, 1850–1856.
12. Mammucari, C., Tommasi di Vignano, A., Sharov, A.A., Neilson, J., Havrda, M.C., Roop, D.R., Botchkarev, V.A., Crabtree, G.R. and Dotto, G.P. (2005) Integration of Notch 1 and calcineurin/NFAT signaling pathways in keratinocyte growth and differentiation control. *Dev. Cell*, **8**, 665–676.
13. Strippoli, P., Petrini, M., Lenzi, L., Carinci, P. and Zannotti, M. (2000) The murine DSCR1-like (Down syndrome candidate region 1) gene family: conserved synteny with the human orthologous genes. *Gene*, **257**, 223–232.
14. Crawford, D.R., Leahy, K.P., Abramova, N., Lan, L., Wang, Y. and Davies, K.J. (1997) Hamster adapt78 mRNA is a Down syndrome critical region homologue that is inducible by oxidative stress. *Arch. Biochem. Biophys.*, **342**, 6–12.

15. Davies, K.J., Harris, C.D. and Ermak, G. (2001) The essential role of calcium in induction of the DSCR1 (ADAPT78) gene. *Biofactors*, **15**, 91–93.
16. Leahy, K.P., Davies, K.J., Dull, M., Kort, J.J., Lawrence, K.W. and Crawford, D.R. (1999) adapt78, a stress-inducible mRNA, is related to the glucose-regulated protein family of genes. *Arch. Biochem. Biophys.*, **368**, 67–74.
17. Cook, C.N., Hejna, M.J., Magnuson, D.J. and Lee, J.M. (2005) Expression of calcipressin1, an inhibitor of the phosphatase calcineurin, is altered with aging and Alzheimer's disease. *J. Alzheimers Dis.*, **8**, 63–73.
18. Ermak, G., Morgan, T.E. and Davies, K.J. (2001) Chronic overexpression of the calcineurin inhibitory gene DSCR1 (Adapt78) is associated with Alzheimer's disease. *J. Biol. Chem.*, **276**, 38787–38794.
19. Ermak, G., Harris, C.D. and Davies, K.J. (2002) The DSCR1 (Adapt78) isoform 1 protein calcipressin 1 inhibits calcineurin and protects against acute calcium-mediated stress damage, including transient oxidative stress. *FASEB J.*, **16**, 814–824.
20. Leahy, K.P. and Crawford, D.R. (2000) adapt78 protects cells against stress damage and suppresses cell growth. *Arch. Biochem. Biophys.*, **379**, 221–228.
21. Ma, H., Xiong, H., Liu, T., Zhang, L., Godzik, A. and Zhang, Z. (2004) Aggregate formation and synaptic abnormality induced by DSCR1. *J. Neurochem.*, **88**, 1485–1496.
22. Chang, K.T., Shi, Y.J. and Min, K.T. (2003) The Drosophila homolog of Down's syndrome critical region 1 gene regulates learning: implications for mental retardation. *Proc. Natl. Acad. Sci. USA*, **100**, 15794–15799.
23. Chang, K.T. and Min, K.T. (2005) Drosophila melanogaster homolog of Down syndrome critical region 1 is critical for mitochondrial function. *Nat. Neurosci.*, **8**, 1577–1585.
24. Cano, E., Canellada, A., Minami, T., Iglesias, T. and Redondo, J.M. (2005) Depolarization of neural cells induces transcription of the Down syndrome critical region 1 isoform 4 via a calcineurin/nuclear factor of activated T cells-dependent pathway. *J. Biol. Chem.*, **280**, 29435–29443.
25. Groth, R.D. and Mermelstein, P.G. (2003) Brain-derived neurotrophic factor activation of NFAT (nuclear factor of activated T-cells)-dependent transcription: a role for the transcription factor NFATc4 in neurotrophin-mediated gene expression. *J. Neurosci.*, **23**, 8125–8134.
26. Graef, I.A., Wang, F., Charron, F., Chen, L., Neilson, J., Tessier-Lavigne, M. and Crabtree, G.R. (2003) Neurotrophins and netrins require calcineurin/NFAT signaling to stimulate outgrowth of embryonic axons. *Cell*, **113**, 657–670.
27. Lin, H.Y., Michtalik, H.J., Zhang, S., Andersen, T.T., Van Riper, D.A., Davies, K.K., Ermak, G., Petti, L.M., Nachod, S., Narayan, A.V. *et al*. (2003) Oxidative and calcium stress regulate DSCR1 (Adapt78/MCIP1) protein. *Free Radic. Biol. Med.*, **35**, 528–539.
28. Michtalik, H.J., Narayan, A.V., Bhatt, N., Lin, H.Y., Mulligan, M.T., Zhang, S.L. and Crawford, D.R. (2004) Multiple oxidative stress-response members of the Adapt78 family. *Free Radic. Biol. Med.*, **37**, 454–462.
29. See, V. and Loeffler, J.P. (2001) Oxidative stress induces neuronal death by recruiting a protease and phosphatase-gated mechanism. *J. Biol. Chem.*, **276**, 35049–35059.
30. Cho, Y.J., Abe, M., Kim, S.Y. and Sato, Y. (2005) Raf-1 is a binding partner of DSCR1. *Arch. Biochem. Biophys.*, **439**, 121–128.
31. Goll, D.E., Thompson, V.F., Li, H., Wei, W. and Cong, J. (2003) The calpain system. *Physiol. Rev.*, **83**, 731–801.
32. Minami, T., Horiuchi, K., Miura, M., Abid, M.R., Takabe, W., Noguchi, N., Kohro, T., Ge, X., Aburatani, H., Hamakubo, T. *et al*. (2004) Vascular endothelial growth factor- and thrombin-induced termination factor, Down syndrome critical region-1, attenuates endothelial cell proliferation and angiogenesis. *J. Biol. Chem.*, **279**, 50537–50554.
33. Alemany, R. and Curiel, D.T. (2001) CAR-binding ablation does not change biodistribution and toxicity of adenoviral vectors. *Gene Ther.*, **8**, 1347–1353.
34. Kaneko, S., Kawakami, S., Hara, Y., Wakamori, M., Itoh, E., Minami, T., Takada, Y., Kume, T., Katsuki, H., Mori, Y. *et al*. (2006) A critical role of TRPM2 in neuronal cell death by hydrogen peroxide. *J. Pharmacol. Sci.*, **101**, 66–76.
35. Hara, Y., Wakamori, M., Ishii, M., Maeno, E., Nishida, M., Yoshida, T., Yamada, H., Shimizu, S., Mori, E., Kudoh, J. *et al*. (2002) LTRPC2 Ca2 + -permeable channel activated by changes in redox status confers susceptibility to cell death. *Mol. Cell*, **9**, 163–173.
36. Montell, C. (2005) The TRP superfamily of cation channels. *Sci. STKE*, **2005**, re3.
37. Hogan, P.G., Chen, L., Nardone, J. and Rao, A. (2003) Transcriptional regulation by calcium, calcineurin, and NFAT. *Genes Dev.*, **17**, 2205–2232.
38. Im, S.H. and Rao, A. (2004) Activation and deactivation of gene expression by Ca2 + /calcineurin-NFAT-mediated signaling. *Mol. Cells*, **18**, 1–9.
39. Kalivendi, S.V., Konorev, E.A., Cunningham, S., Vanamala, S.K., Kaji, E.H., Joseph, J. and Kalyanaraman, B. (2005) Doxorubicin activates nuclear factor of activated T-lymphocytes and Fas ligand transcription: role of mitochondrial reactive oxygen species and calcium. *Biochem. J.*, **389**, 527–539.
40. Huang, C., Li, J., Costa, M., Zhang, Z., Leonard, S.S., Castranova, V., Vallyathan, V., Ju, G. and Shi, X. (2001) Hydrogen peroxide mediates activation of nuclear factor of activated T cells (NFAT) by nickel subsulfide. *Cancer Res.*, **61**, 8051–8057.
41. Benedito, A.B., Lehtinen, M., Massol, R., Lopes, U.G., Kirchhausen, T., Rao, A. and Bonni, A. (2005) The transcription factor NFAT3 mediates neuronal survival. *J. Biol. Chem.*, **280**, 2818–2825.
42. Aramburu, J., Yaffe, M.B., Lopez-Rodriguez, C., Cantley, L.C., Hogan, P.G. and Rao, A. (1999) Affinity-driven peptide selection of an NFAT inhibitor more selective than cyclosporin A. *Science*, **285**, 2129–2133.
43. Abbasi, S., Lee, J.D., Su, B., Chen, X., Alcon, J.L., Yang, J., Kellems, R.E. and Xia, Y. (2006) Protein kinase-mediated regulation of calcineurin through the phosphorylation of modulatory calcineurin-interacting protein 1. *J. Biol. Chem.*, **281**, 7717–7726.
44. Vega, R.B., Rothermel, B.A., Weinheimer, C.J., Kovacs, A., Naseem, R.H., Bassel-Duby, R., Williams, R.S. and Olson, E.N. (2003) Dual roles of modulatory calcineurin-interacting protein 1 in cardiac hypertrophy. *Proc. Natl. Acad. Sci. USA*, **100**, 669–674.
45. Kregel, K.C. and Zhang, H.J. (2007) An integrated view of oxidative stress in aging: basic mechanisms, functional effects, and pathological considerations. *Am. J. Physiol. Regul. Integr. Comp. Physiol.*, **292**, R18–R36.
46. Kamsler, A. and Segal, M. (2003) Hydrogen peroxide modulation of synaptic plasticity. *J. Neurosci.*, **23**, 269–276.
47. Asai, A., Qiu, J., Narita, Y., Chi, S., Saito, N., Shinoura, N., Hamada, H., Kuchino, Y. and Kirino, T. (1999) High level calcineurin activity predisposes neuronal cells to apoptosis. *J. Biol. Chem.*, **274**, 34450–34458.
48. Lee, B., Butcher, G.Q., Hoyt, K.R., Impey, S. and Obrietan, K. (2005) Activity-dependent neuroprotection and cAMP response element-binding protein (CREB): kinase coupling, stimulus intensity, and temporal regulation of CREB phosphorylation at serine 133. *J. Neurosci.*, **25**, 1137–1148.
49. Wang, H.G., Pathan, N., Ethell, I.M., Krajewski, S., Yamaguchi, Y., Shibasaki, F., McKeon, F., Bobo, T., Franke, T.F. and Reed, J.C. (1999) Ca2 + -induced apoptosis through calcineurin dephosphorylation of BAD. *Science*, **284**, 339–343.
50. Springer, J.E., Azbill, R.D., Nottingham, S.A. and Kennedy, S.E. (2000) Calcineurin-mediated BAD dephosphorylation activates the caspase-3 apoptotic cascade in traumatic spinal cord injury. *J. Neurosci.*, **20**, 7246–7251.
51. Kakita, T., Hasegawa, K., Iwai-Kanai, E., Adachi, S., Morimoto, T., Wada, H., Kawamura, T., Yanazume, T. and Sasayama, S. (2001) Calcineurin pathway is required for endothelin-1-mediated protection against oxidant stress-induced apoptosis in cardiac myocytes. *Circ. Res.*, **88**, 1239–1246.
52. De Windt, L.J., Lim, H.W., Taigen, T., Wencker, D., Condorelli, G., Dorn, G.W., 2nd., Kitsis, R.N. and Molkentin, J.D. (2000) Calcineurin-mediated hypertrophy protects cardiomyocytes from apoptosis *in vitro* and *in vivo*: An apoptosis-independent model of dilated heart failure. *Circ. Res.*, **86**, 255–263.
53. Bueno, O.F., Lips, D.J., Kaiser, R.A., Wilkins, B.J., Dai, Y.S., Glascock, B.J., Klevitsky, R., Hewett, T.E., Kimball, T.R., Aronow, B.J. *et al*. (2004) Calcineurin Abeta gene targeting predisposes the myocardium to acute ischemia-induced apoptosis and dysfunction. *Circ. Res.*, **94**, 91–99.
54. Sanna, B., Brandt, E.B., Kaiser, R.A., Pfluger, P., Witt, S.A., Kimball, T.R., van Rooij, E., De Windt, L.J., Rothenberg, M.E., Tschop, M.H. *et al*. (2006) Modulatory calcineurin-interacting proteins 1 and 2 function as calcineurin facilitators *in vivo*. *Proc. Natl. Acad. Sci. USA*, **103**, 7327–7332.

55. Ryeom, S., Greenwald, R.J., Sharpe, A.H. and McKeon, F. (2003) The threshold pattern of calcineurin-dependent gene expression is altered by loss of the endogenous inhibitor calcipressin. *Nat. Immunol.*, **4**, 874–881.
56. Wiese, A.G., Pacifici, R.E. and Davies, K.J. (1995) Transient adaptation of oxidative stress in mammalian cells. *Arch. Biochem. Biophys.*, **318**, 231–240.
57. Feliubadaló, L., Arbonés, M.L., Manas, S., Chillaron, J., Visa, J., Rodes, M., Rousaud, F., Zorzano, A., Palacin, M. and Nunes, V. (2003) Slc7a9-deficient mice develop cystinuria non-I and cystine urolithiasis. *Hum. Mol. Genet.*, **12**, 2097–2108.
58. Fujita, Y., Katagi, J., Tabuchi, A., Tsuchiya, T. and Tsuda, M. (1999) Coactivation of secretogranin-II and BDNF genes mediated by calcium signals in mouse cerebellar granule cells. *Brain Res. Mol. Brain Res.*, **63**, 316–324.
59. Pfaffl, M.W. (2001) A new mathematical model for relative quantification in real-time RT–PCR. *Nucleic Acids Res.*, **29**, e45.
60. Becker, T.C., Noel, R.J., Coats, W.S., Gomez-Foix, A.M., Alam, T., Gerard, R.D. and Newgard, C.B. (1994) Use of recombinant adenovirus for metabolic engineering of mammalian cells. *Methods Cell Biol.*, **43**, 161–189.
61. Venables, W.N. (2002) *Modern Applied Statistics with S*. Sringer-Verlag, New York.
62. Good, P.I. (1994) *Permutation Tests for Testing Hypotheses*. Springer-Verlag, New York.